Viscoelasticity imaging of biological tissues with phase-resolved photoacoustic measurement

Guodong Gao,† Sihua Yang,† and Da Xing*

MOE Key Laboratory of Laser Life Science & Institute of Laser Life Science, College of Biophotonics, South China Normal University, Guangzhou 510631, China

**Corresponding author: xingda@scnu.edu.cn*

Received May 25, 2011; revised July 26, 2011; accepted July 27, 2011; posted August 2, 2011 (Doc. ID 148209); published August 19, 2011

A method for noninvasive viscoelasticity imaging of biological tissues using phase-resolved photoacoustic measurement is presented. We deduced the process of photoacoustic effect on the basis of thermal viscoelasticity theory, and established the relationship between the photoacoustic phase delay and the viscosity–elasticity ratio for soft solids. Agar phantoms with different densities and different absorption coefficients were used to verify the dependence of photoacoustic phase-resolved viscoelasticity measurements. Moreover, viscoelasticity imaging of tissues was obtained with a photoacoustic point scanning system. The photoacoustic phase-resolved method provides a basis for viscoelasticity imaging, which can potentially be used for detection of viscoelastic properties and lesions of biological tissues.

OCIS codes: 120.5050, 170.5120, 170.6935.

The elastic property is an important physically characterized parameter closely connected to the thermodynamic properties of materials, whose changes in biological tissues are often related to pathology [1–3]. However, most biological tissues show viscoelastic characterization and rheological behavior in the human body. A soft solid, such as cartilage, bone, tendon, and muscle, requires both viscosity and elasticity information simultaneously to describe its mechanical behavior [4,5]. It is not comprehensive and inaccurate to just use the elastic property to express the intrinsic characteristics of biological tissues [6,7]. Therefore, a detection technique to characterize viscoelasticity of tissues would be great progress in medical applications and clinical research.

Photoacoustic (PA) imaging is an emerging imaging modality under preclinical development that has been applied to several biomedical applications for obtaining structural and functional information [8–10]. The PA effect refers to the generation of an acoustic wave by the absorption of electromagnetic energy, such as laser or radio-frequency waves [11]. By reason of the viscoelasticity of tissue, there is a phase lag when PA waves launch from the thermal expansion source caused by the excitation laser. Different tissue types or pathologies with corresponding viscoelastic properties will lead to different phase lags of the PA wave. Therefore, PA viscoelasticity imaging can be obtained based on the contrast with phase delay time.

In this Letter, we theoretically deduced the mathematical relationship between the PA phase delay and the viscosity-elasticity ratio. Moreover, a system to measure the phase delay time of the PA wave generated from different tissues was developed.

An intensity-modulated CW laser was used to radiate absorptive isotropic viscoelastic structures; the light intensity is given by $I = 1/2I_0(1 + \cos \omega t)$, where I_0 is the time-averaged light intensity and ω is the modulation frequency. Light absorption by the absorber results in a sinusoidal temperature variation in the form of $T = T_0 e^{i\omega t}$ due to the nonradiative transition, and then causes thermal expansion and shrinkage as well as PA wave generation based on the thermoelastic mechanism. Because of the cyclical changes of the light intensity, the PA wave whose dominant frequency is equal to the modulated frequency is excited periodically. In the above process, the cyclical heating in the local region induces the thermal stress, and strain generates due to the stress in the form of the force-produced PA waves. Because of the damping effect due to the viscoelasticity of biological tissues, it could be found that the strain also alternated periodically, but would be out of phase with the stress [12].

In fact, the above-mentioned process is a problem of the rheonomous thermal stress caused by a periodically variational point heat source for an unbounded isotropic viscoelastic solid. By resolving this problem, the radial thermal stress in the spherical coordinate system can be expressed as [13]

$$\sigma = -\frac{4G}{r}\frac{\partial \Phi}{\partial r} + \rho \frac{\partial^2 \Phi}{\partial t^2}, \tag{1}$$

where G is Green's function of thermal conduction, Φ is the thermoelastic displacement potential and is defined by $\Delta\Phi = \alpha T(1 + \nu)/(1 - \nu)$, α is the coefficient of linear expansion, and ν is Poisson's ratio. In the condition of temperature $T = T_0 e^{i\omega t}$, the stress σ can be rewritten as [14]

$$\sigma = -E\alpha T_0 e^{i\omega t}/(1 - \nu), \tag{2}$$

where E is Young's modulus and ω is the modulation frequency. In the rheological Kelvin–Voigt model, the constitutive equation in terms of a stress–strain relationship can be expressed as [12,14]

$$\sigma = E\varepsilon + \eta\dot{\varepsilon}. \tag{3}$$

Combining Eqs. (2) and (3), we have [12,15]

$$\varepsilon(t) = \varepsilon_A e^{i(\omega t + \delta)}, \tag{4}$$

$$\delta = \arctan\frac{\eta\omega}{E}, \tag{5}$$

where $\varepsilon_A = (-E^2\alpha T)/[(E^2+\eta^2\omega^2)\cos\delta(1-\nu)]$ is the amplitude of the complex strain. The physical significance of Eq. (4) indicates that δ is the phase delay of the strain response to the stress. From Eq. (5), we can see the relationship between the phase delay δ and the viscosity-elasticity ratio η/E.

The experimental schematic diagram is shown in Fig. 1. A CW laser with a wavelength of 808 nm was used as excitation source. The intensity of the CW laser was modulated by the electro-optic (E-O) light modulator with a 90% modulation depth at a frequency of 50 KHz. The modulation signal applied to the voltage amplifier attached to the modulator from the function generator was equal to the center frequency of the ultrasonic transducer. A lock-in amplifier was used to detect the dominant frequency of the PA wave and calculate the phase lag between the dominant frequency PA wave and the reference signal. Samples were made into slices with a thickness of 0.3 mm. A laser through an optical lens illuminated the target at a focal point of about 0.1 mm. The laser power density on the sample surface was limited to 200 $\mathrm{mW/cm^2}$. The transducer was placed against the laser and fastened to a two-dimensional scan platform, which moved point by point with a step distance of 100 μm and a total scan range of 5 mm. As shown in the dashed box in Fig. 1, the sample and the transducer were fixed together and the distance from the light spot to the transducer was kept strictly consistent when the sample was changed.

Actually, the phase measured by the above system is the phase difference δ_m between the PA signal and the reference signal used to modulate the laser. Except for the phase delay δ in Eq. (5), the phase difference δ_m also includes the relaxation time δ_t for the nonradiative transition and the delay time δ_s caused by system. Therefore, we have

$$\delta_m = \delta_t + \delta_s + \delta. \tag{6}$$

The order of magnitude of relaxation time δ_t is about 10^{-11} s [16]. It can be ignored when the modulation frequency is 5×10^4 Hz in the experiment for the phase delay $\delta \gg \delta_t$. Although the delay time δ_s caused by the system is difficult to measure precisely, it is stable in the same system and could be treated as a constant. So the magnitude of δ_m is considered to be only correlated with δ in the experiment.

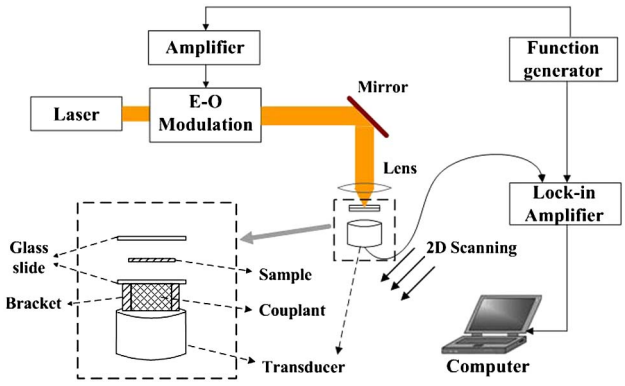

Fig. 1. (Color online) Scheme of experimental setup for PA viscoelasticity imaging system.

In order to verify the dependence of the PA phase delay on the viscoelastic property within our system, six agar phantoms with different densities of 0.6%, 1.2%, 1.8%, 2.4%, 3.0%, and 3.6% were used to simulate tissues with different viscoelastic properties. As predicted theoretically, the observed phase delay between the dominant frequency of the PA wave and the modulation signal increased with the increase in density of the sample. Figure 2(a) demonstrates the comparison between the results from the PA experiment and the data measured with the rheometer [15]. The variation tendency of the phase delay obtained by the PA measurement agreed well with the internal friction angle measured using the rheometer. The fitting lines of the two groups' data are parallel in general, which indicated that the variation of the PA phase delay was related to the viscoelastic properties of materials and the theory we proposed was reasonable to explain the phenomenon of PA phase delay. The intercept of two fitting lines was mainly the sum of the delay time δ_s caused by the system and the relaxation time δ_t of the nonradiative transition. Additionally, the influence on the PA phase delay of the absorption coefficient was taken into account. Agars with different absorption coefficients but the same density were controlled by the interfusing of ink with a proportion of 2%, 4%, and 6%, respectively. According to the results shown in Fig. 2(b), the measured PA phase delays are almost the same in every density, which indicates that the absorption coefficient has little impact on PA phase delay but determines the PA intensity as shown in Fig. 2(c).

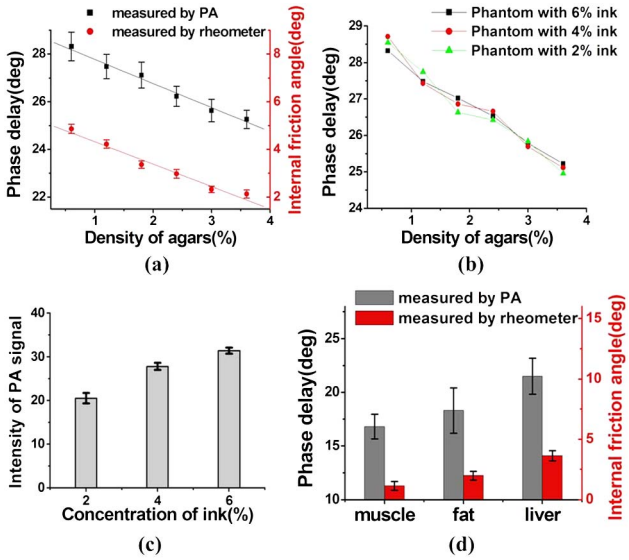

Fig. 2. (Color online) (a) Comparison between the phase delay of the PA wave and the internal friction angle measured by rheometer. The values of phase delay were averaged over 16 tests. (b) Phase delay obtained by PA measurement from agars with different absorption coefficients. (c) PA intensity of the agar phantoms with different proportions of ink. (d) Comparison between the phase delay of the PA wave and the internal friction angle measured by rheometer for biological tissues.

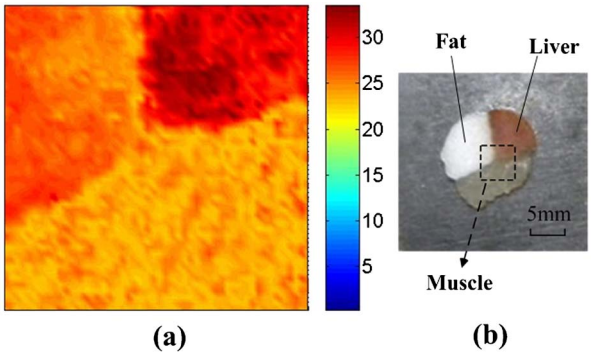

Fig. 3. (Color online) (a) PA viscoelasticity imaging of sample. (b) Photograph of sample; the dashed frame is the PA scanning area.

To verify the feasible of PA viscoelasticity imaging of tissues, three biological samples (muscle, fat, and liver from a pig) were tested by the method shown in Fig. 2. The measured results of the PA phase delay shown in Fig. 2(d) demonstrated the liver tissue had a higher viscosity–elasticity ratio than fat and muscle, which variation tendency was also well matched with the data measured by the rheometer. Furthermore, PA viscoelasticity imaging of biological tissues was performed with point by point scanning. The imaging sample and the scanning area are shown in Fig. 3(b). The PA phase delay measured from each scanning point was projected to image the relative viscoelasticity distribution. The reconstruction image is shown in Fig. 3(a), and the color bar represents the relative viscosity–elasticity ratio. The image clearly revealed the boundary of the composite sample and the imaging intensity for distinguishing different tissues. The results demonstrated that PA viscoelasticity imaging can be used to characterize the biomechanical property of biological tissues.

The accuracy of the measurement system was limited by the time constant of the lock-in amplifier and the signal-to-noise ratio (SNR). A longer time constant will improve the performance but reduce the scanning speed and SNR. A value of 300 ms time constant is selected to perform experiments, which is the main reason for the uneven distribution of the pixel values in Fig. 3. The acquisition time required for Fig. 3(a) is about 45 min, which would be reduced by improving the parameter of the stepper motor and enhancing the sensitivity of the transducer. Besides, in the opposite pattern of excitation and receiving, the thickness and sound velocity of the sample would lead to comparison error among different samples in our experiments. The sound velocity differences in the three tissues (Fig. 3) have orders of magnitude of 10 m/s. The PA phase error caused by the velocity differences is calculated to be smaller than 0.1 deg when the sample thickness is 0.3 mm. Additionally, phase-wrapping might be involved in the phase measurement when using a high frequency transducer at the present detection configuration. In the future, a bowl-shaped transducer will be fabricated and an acousto-opitc confocal detection mode would be adopted to increase SNR. The reflection mode with illumination and ultrasonic detection from the same side will be necessary to avoid the phase error resulting from the ultrasound path difference and the phase wrapping, which is convenient to realize *in vivo* measurements. Moreover, depth scanning for different types of tissue will also be tried by adjusting the focus of incident light.

In summary, we have proposed a method for noninvasive characterization of the biological tissue viscoelasticity with PA phase-resolved measurements. The theory approaches the problem of the PA effect on the basis of thermal stress to explain the PA phase delay phenomenon. A system of PA viscoelasticity imaging was developed, and the high contrast image reflecting the tissue viscoelasticity information with the PA phase projection was successfully achieved. Diagnostic detection of an atherosclerotic plaque and skin tumor would be the most promising application of the technique, which are sensitive to the viscoelastic properties of tissue. It is trusted that PA viscoelasticity imaging would have great potential application in both biomedical research and clinical study.

This research is supported by the National Basic Research Program of China (2011CB910402, 2010CB732602), the Program for Changjiang Scholars and Innovative Research Team in University (IRT0829), the National Natural Science Foundation of China (NSFC) (30870676), and the Foundation for Distinguished Young Talents in Higher Education of Guangdong, China (LYM10061).

†Both authors contributed equally to this work.

References

1. J. Ophir, I. Cespedes, H. Ponnenkanti, Y. Yazdi, and X. Li, Ultrason. Imag. **13**, 111 (1991).
2. R. Muthupillai, D. J. Lomas, P. J. Rossman, J. F. Greenleaf, and R. L. Ehman, Science **269**, 1854 (1995).
3. S. G. Adie, X. Liang, B. F. Kennedy, R. John, D. D. Sampson, and S. A. Boppart, Opt. Express **18**, 25519 (2010).
4. I. S. Kovach, Biophys. Chem. **59**, 61 (1996).
5. V. C. Mow, A. Ratcliffe, and A. R. Poole, Biomaterials **13**, 67 (1992).
6. R. M. Lerner, S. R. Huang, and K. J. Parker, Ultrasound Med. Biol. **16**, 231 (1990).
7. M. Fatemi and J. F. Greenleaf, Science **280**, 82 (1998).
8. Y. Yuan, S. H. Yang, and D. Xing, Opt. Lett. **35**, 2266 (2010).
9. S. H. Yang, D. Xing, Y. Q. Lao, D. W. Yang, L. M. Zeng, L. Zh. Xiang, and W. R. Chen, Appl. Phys. Lett. **90**, 243902 (2007).
10. F. Ye, S. H. Yang, and D. Xing, Appl. Phys. Lett. **97**, 213702 (2010).
11. L. Song, K. Maslov, and L. V. Wang, Opt. Lett. **35**, 1482 (2010).
12. J. D. Ferry, *Viscoelastic Properties of Polymers* (Wiley, 1980).
13. Y. Takeuchi, *Thermal Stress* (Science, 1978).
14. A. F. Mak, W. M. Lai, and V. C. Mow, J. Biomech. **20**, 703 (1987).
15. H. A. Baraes, J. F. Hutton, and K. Walters, *An Introduction to Rheology* (Elsevier, 1989).
16. J. L. Jiménez Pérez, A. Cruz-Orea, E. Ramón-Gallegos, R. Gutierrez Fuentes, and J. F. Sanchez Ramirez, Eur. J. Phys. Special Topics **153**, 353 (2008).